Materials Research Bulletin 89 (2017) 180–184

Contents lists available at ScienceDirect

Materials Research Bulletin

journal homepage: www.elsevier.com/locate/matresbu

Strain fluctuations in $BaTiO_3/SrTiO_3$ heterostructures

V. Gartnerova[a], O. Pacherova[b], M. Klinger[a], M. Jelinek[b], A. Jager[a], M. Tyunina[b,c,*]

[a] Laboratory of Nanostructures and Nanomaterials, Institute of Physics, CAS, Na Slovance 2, 182 21 Prague, Czechia
[b] Institute of Physics, CAS, Na Slovance 2, 182 21 Prague, Czechia
[c] Microelectronics Research Unit, Faculty of Information Technology and Electrical Engineering, University of Oulu, P.O. Box 4500, FI-90014, Finland

ARTICLE INFO

Article history:
Received 26 June 2016
Received in revised form 8 December 2016
Accepted 31 January 2017
Available online 1 February 2017

Keywords:
A. Oxides
A. Thin films
B. Epitaxial growth
C. Electron microscopy
C. X-ray diffraction

ABSTRACT

Epitaxy of perovskite oxide ferroelectric heterostructures with large lattice misfit is crucial for numerous emerging applications. Here we demonstrate cube-on-cube-type epitaxial growth of $BaTiO_3$ films on strongly mismatched (001)$SrTiO_3$ single-crystal substrates for the films with thicknesses significantly larger than that of misfit relaxation. The films experience strain originating from the film-substrate thermal expansion mismatch. Using a dedicated digital analysis of electron microscopy images, we show that the films contain random nanoregions of substantial strain fluctuations: the local strains vary in the range of ~(0.5–2)% compared with the average strain magnitude of ~1%. Because of strong strain-polarization coupling in ferroelectrics, fluctuations of strain produce fluctuations of polarization, which are suggested to cause relaxor-like properties in many mismatched heterostructures.

1. Introduction

Barium titanate ($BaTiO_3$, BTO) is an archetypical representative of perovskite-type oxide ferroelectrics [1–4]. Strong coupling between lattice strain and electrical polarization is responsible for numerous effects and unique properties of ferroelectrics enabling a variety of applications of these materials in their bulk form. Likewise, single-crystal-type epitaxial ferroelectric films are envisaged to enable numerous emerging applications. Moreover, the strain-polarization coupling makes it possible to control ferroelectric phases, phase transitions, polarization, and related response functions by varying lattice strain in epitaxial films. For heteroepitaxial films, large lattice strains can be caused by misfit between crystal symmetries, lattice parameters, and thermal expansion coefficients of the film and substrate materials. In particular, a cube-on-cube-type epitaxial ferroelectric film grown on top of a cubic substrate can experience biaxial in-plane (parallel to the substrate surface) misfit strain $s = a_s/a_f - 1$, where a_s and a_f are the lattice parameters of the substrate and unstressed film materials, correspondingly. The theoretical strain-temperature *s-T* phase diagrams of epitaxial ferroelectric films were first proposed almost two decades ago [5]. In particular, it was predicted that crystal phases, ferroelectric phases, and phase transitions in epitaxial BTO films experiencing substrate-induced strain can differ significantly from those in bulk single-crystal BTO [5,6]. Also compared with bulk, the polarization can be enhanced in the strained epitaxial films [7,8].

There is, however, a restriction to epitaxy. Indeed, elastic energy of a strained epitaxial film increases with increasing film's thickness. When thickness reaches a critical one, the strain starts relaxing [9]. Often, the critical thickness is theoretically estimated considering complete relaxation of strain through formation of misfit dislocations [9]. The critical thickness decreases from ~100 nm to ~(2–4) nm with increasing strain magnitude from 1% to 2.5% in perovskite oxide ferroelectric films. It means that the misfit strain can relax gradually during film growth, resulting in a distribution of strain across the thickness of the film, or in the vertical bottom-to-top direction. The residual strain is believed to monotonically decrease towards the top of the film [10]. The corresponding smooth, continuous strain gradient, which is formed additionally to the average strain, can further modify the *s-T* phase diagram and properties of ferroelectric films through flexoelectric effect [11–13].

Besides the formation of dislocations and gradual relaxation of strain, also other routes for strain relaxation exist. In particular, specific domain configurations, morphological instabilities, and defects other than dislocations assist strain relaxation [14–20]. Along with the average strain and monotonic inhomogeneous strain, also local fluctuations of lattice strain can principally exist in the films [21].

* Corresponding author at: Microelectronics Research Unit, Faculty of Information Technology and Electrical Engineering, University of Oulu, P.O. Box 4500, FI-90014, Finland.
E-mail address: marinat@ee.oulu.fi (M. Tyunina).

http://dx.doi.org/10.1016/j.materresbull.2017.01.048
0025-5408/

Importantly, epitaxial films for future devices should be integrated with other films and substrates, required by applications rather than determined by perfect epitaxial match. Thus, possibility for epitaxial growth of strongly mismatched ferroelectric films and knowledge of lattice strain therein are of high practical importance. Here we experimentally demonstrate epitaxy of BTO onto strongly mismatched $SrTiO_3$ (STO) substrates for BTO thickness exceeding the critical one. We also show that nanometer-size regions possessing different strains are formed in such films.

2. Experiment

Heteroepitaxial (50–100)-nm-thick BTO films were grown on $SrTiO_3$ (001) (STO) single-crystal substrates (MTI Corp., USA). The films were grown by pulsed laser deposition (PLD) at the substrate temperature of 973 K and oxygen pressure of 20 Pa, which was raised to 800 Pa during post deposition cooling. Compared to typical conditions for PLD of BTO, the oxygen pressure maintained here is very high, which ensures proper oxygen stoichiometry and prevents the formation of dipolar defects in BTO [22].

The crystal structure of the films was studied by x-ray diffraction (XRD) on a Bruker D8 DISCOVER SUPER SPEED SOLUTION diffractometer using Cu-Kα radiation. The Θ-2Θ scans in the range of $2\Theta = 10–130°$ and reciprocal space maps (RSM) in the vicinity of the perovskite (002), (004), (303), (113), and (311) diffractions were measured at room-temperature. The in-plane (parallel to substrate surface) and out-of-plane (normal to substrate surface) lattice parameters were estimated from the positions of films' diffractions using EVA software and taking substrates as a reference.

The local crystal structure was inspected by transmission electron microscopy (TEM) and high-resolution transmission electron microscopy (HRTEM) using a FEI Tecnai TF20 X-twin microscope operated at 200 kV. Cross-sectional samples for the analysis were prepared by focused ion beam (FIB) milling on Dual-Beam scanning electron microscope FEI Quanta 3D FEG equipped with Ga+ FIB. The bright-field TEM (BF-TEM), selected area electron diffraction (SAED), and HRTEM imaging combined with fast Fourier transforms (FFT) and Fourier filtering were employed in order to investigate epitaxy, defects, and strain state in BTO.

A special procedure was applied in order to quantify spatial distribution of lattice parameters. The HRTEM images with the field of view ~(20 nm × 20 nm) were acquired along the [100] axis of BTO. The images overlapped and covered the whole film in the out-of-plane direction. The (010) and (001) interplanar distances, corresponding to the in-plane and out-of-plane lattice parameters of BTO, were extracted from fast Fourier transforms of the images using sliding-window technique and CrysTBox diffractGUI software [23–25]. The dimensions of the windows were set to ~5 nm in the out-of-plane direction and ~20 nm in the in-plane direction, which ensured high accuracy with sufficient spatial resolution in the out-of-plane direction. The lattice parameters were estimated as a function of distance x from the bottom of the film using averaging and binning of the data extracted from each of the windows.

3. Results and discussion

The BTO-STO lattice misfit is large, ~2.7% [26]. Correspondingly, the critical thickness for relaxation of misfit strain is small, a few nanometers only, in BTO on STO [17,18,27]. Despite the large misfit and small critical thickness, epitaxial growth of the BTO films with thicknesses to 100 nm is achieved on STO. Epitaxy is evidenced by XRD and TEM/HRTEM analyses. The BTO films are perovskite, highly oriented, with the (00l) planes parallel to the (001) STO substrate surface [Fig. 1].

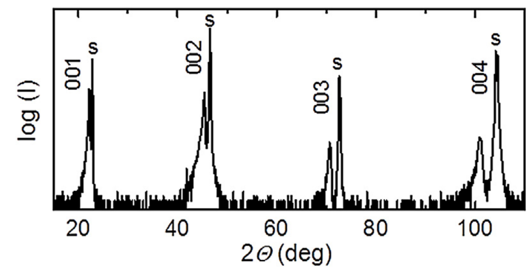

Fig. 1. X-ray diffraction Θ-2Θ scan. Substrate diffractions are marked by s.

The crystal structure of the films can be initially interpreted as pseudo-cubic. A cube-on-cube-type epitaxial growth is revealed by RSM analysis [Fig. 2]. The epitaxial relationship is [100](001)BTO || STO [100](001). Structural domains with other crystal orientations are not detected in the films.

The measured out-of-plane lattice parameter of BTO is $c_f = 0.3996$ nm, and the in-plane lattice parameters are $a_f = b_f = 0.4026$ nm. Compared with the room-temperature lattice parameters $a = b = 0.3992$ nm and $c = 0.4036$ nm of the tetragonal bulk BTO phase [26], the films experience anisotropic lattice strain. The in-plane strain is tensile $s_a = a_f/a - 1 \approx 0.9\%$, and the out-of-plane strain is compressive $s_c = c_f/c - 1 \approx -1\%$ in the films. The BTO-STO lattice mismatch suggests a theoretical in-plane *compressive* misfit strain in BTO [26]. The detected large in-plane *tensile* strain implies that the expected compressive misfit strain is relaxed. The relaxation of misfit strain is consistent with the previously found critical thickness for strain relaxation being ~(2–4) nm only in the BTO films on STO [17,18,27]. The misfit strain is relaxed in the vicinity of the BTO-STO interface during the high-temperature growth of BTO. The room-temperature strain state results from the post-deposition cooling and corresponding build-up of thermal strain in the BTO film. The thermal strain arises from the mismatch existing between coefficients of thermal expansion in BTO and STO [26]. The room-temperature in-plane tensile thermal strain in the BTO film on STO is consistent with the theoretical model [28].

Additionally to the average (or homogeneous) strain determined from the positions of perovskite diffractions, a distribution of strain (or inhomogeneous strain) is detected by inspections of the diffractions' widths. The full width at half maximum, w, is determined for the (00l) diffractions in the Cu Kα_1 Θ-2Θ scans. The widths are analysed using the Williamson-Hall approach. The shape of diffractions is found to be best fitted by a Gaussian peak [Fig. 3(a)]. Hence, the Williamson-Hall plot of $A^2 = (w\cos\Theta/\lambda)^2$ versus $(\sin\Theta/\lambda)^2$ is employed, where λ is the wavelength of the Cu Kα_1 radiation. The obtained good linear fit [Fig. 3(b)] indicates the presence of inhomogeneous strain in the film. The coherence length extracted from the linear fit is ~60 nm for the 70-nm-thick

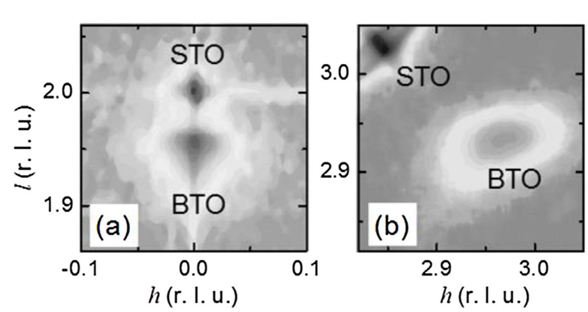

Fig. 2. Reciprocal space maps (a) for (002) and (b) for (303) directions. The results are presented in reciprocal lattice units (r.l.u.) of STO.